Possible "Magnéli" Phases and Self-Alloying in the Superconducting Sulfur Hydride

Ryosuke Akashi,[1,*] Wataru Sano,[2,3] Ryotaro Arita,[3,4] and Shinji Tsuneyuki[1,5]
[1]Department of Physics, The University of Tokyo, Hongo, Bunkyo-ku, Tokyo 113-0033, Japan
[2]Department of Applied Physics, The University of Tokyo, Hongo, Bunkyo-ku, Tokyo 113-8656, Japan
[3]RIKEN Center for Emergent Matter Science, Wako, Saitama 351-0198, Japan
[4]JST ERATO Isobe Degenerate π-Integration Project, Advanced Institute for Materials Research (AIMR), Tohoku University, Sendai, Miyagi 980-8577, Japan
[5]Institute of Solid State Physics, The University of Tokyo, Kashiwa, Chiba 277-8581, Japan
(Received 17 December 2015; published 10 August 2016)

We theoretically give an infinite number of metastable crystal structures for the superconducting sulfur hydride H_xS under pressure. Previously predicted crystalline phases of H_2S and H_3S have been thought to have important roles for experimentally observed low and high T_c, respectively. The newly found structures are long-period modulated crystals where slablike H_2S and H_3S regions intergrow on a microscopic scale. The extremely small formation enthalpy for the H_2S-H_3S boundary indicated by first-principles calculations suggests possible alloying of these phases through the formation of local H_3S regions. The modulated structures and gradual alloying transformations between them not only explain the peculiar pressure dependence of T_c in sulfur hydride observed experimentally, but also could prevail in the experimental samples under various compression schemes.

DOI: 10.1103/PhysRevLett.117.075503

Sulfur hydride has recently been found to become a superconductor at an extremely high pressure around 200 K [1,2]. This is the first achievement of a superconducting transition temperature (T_c) exceeding the nitrogen boiling point among the conventional phonon-mediated superconductors [3], and it has broken the long-standing record of 160 K in a mercury cuprate [4–7].

A remarkable feature observed in this superconducting phenomenon is the pressure and annealing-scheme dependences of T_c [1,2,8]. (i) When the pressure ($> \sim$100 GPa) is applied to the H_2S sample at room temperature and afterwards cooled down, the observed T_c's amount to over 150 K, with 203 K being the maximum value (open circle in Fig. 1). (ii) By pressurizing at a temperature around 200 K, on the other hand, the observed T_c remains low and next rapidly increases (open square in Fig. 1). Although this behavior suggests a variety of structural phases and their peculiar properties, efficient experimental observations have been obstructed by the extremely high pressure. Instead, first-principles calculations have provided insights for the superconducting phases. It is now established that some of the observed values of T_c with the low- and high-T schemes are well reproduced [9–17] with crystal structures predicted for compositions of H_2S [9], as well as H_5S_2 [16] and H_3S [10] (see Fig. 1). However, a consistent understanding of the observed behavior still remains unprecedented. In particular, no clear explanation of the rapid increase of T_c with the low-T scheme has been given, despite the accumulated first-principles proposals of candidate structures with various compositions of H_xS [11,14,18,19].

The current theoretical attempts have focused on the possible understanding with a minimal number of distinct structural phases. Rather, we provide a different view: Not only distinct phases but also their mixture have vital roles. Specifically, we find an infinite number of metastable

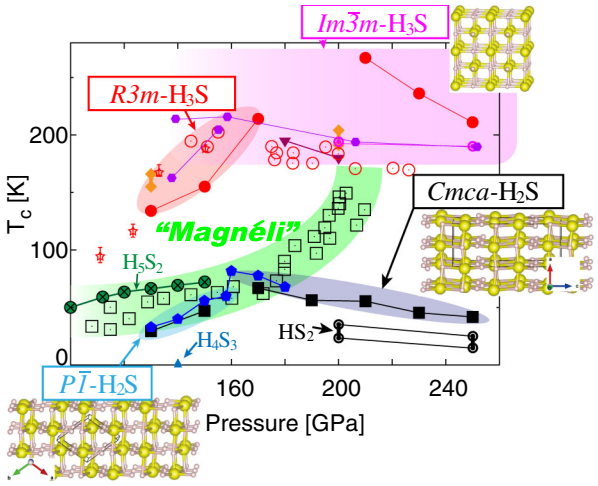

FIG. 1. Experimentally observed T_c (open circle, square [1], and star with an error bar [8]) compared with the first-principles calculations (solid symbols). The latter data are taken from Refs. [9] (pentagon), [10] (rhombus), [12] (inverted triangle), [13] (circle and square), [14] (double circle), [18] (triangle), [15] (hexagon), and [16] (circle with x mark). The data points in the shaded areas have been obtained from the corresponding predicted crystal structures [9,10]. Note that $R3m$-H_3S is a trigonally distorted variant of $Im\bar{3}m$-H_3S. As discussed later, we attribute the pressure dependence of T_c (open square) to the "Magnéli" phases. The values from Ref. [13] (Refs. [14,15]) includes the plasmon effect (phonon anharmonic effect). The vertical bars connecting the rhombi indicate the T_c variation with the empirical Coulomb parameter μ^* [10,14].

crystal structures having compositions H_xS_{1-x} with $2/3 < x < 3/4$, which have not been reported in the first-principles structure-search studies. They can be understood as long-period modulated crystals formed by stacking the H_2S and H_3S slablike structures, which are reminiscent of the Magnéli phases in transition-metal oxides [20]. All these structures are thermodynamically as stable as the complete separation to H_2S and H_3S phases. This suggests that the microscopic *intergrowth* of the H_2S and H_3S regions requires little activation enthalpy and therefore occurs ubiquitously in the experimental situation, forming, as it were, slab-alloy phases. We also show that the experimentally observed T_c-pressure curve is reproduced from these alloylike phases.

We begin with a discussion of the hidden similarity between theoretically predicted relevant structures for H_2S and H_3S. $P\bar{1}$-H_2S and $Cmca$-H_2S (Fig. 1) are known to give low T_c values [9,13,17], which agree relatively well with the experimental values with the low-T annealing for the low-pressure regime. $Im\bar{3}m$-H_3S (Fig. 1) has been thought to give the T_c with the high-T annealing cases [11,14,15,17,21–31], and its presence was recently confirmed with x-ray diffraction measurements [8,18,32,33]. Seen from the $(1\ \ 1\ \ 0)$ direction [$(1\ \ 0\ \ 0)$ direction] in the setup of Ref. [9], one can notice that $P\bar{1}$- and $Cmca$-H_2S can be decomposed into common unit structures [Figs. 2(a) and 2(b)]: two H_2S square nets interlaced with each other [Fig. 2(c)]. The units of this shape are bound with each other so that sulfur atoms adopt local fcc-like stacking [Fig. 2(d)] [34]. The $P\bar{1}$ and $Cmca$ structures can now be distinguished by the configuration of the interunit bonding. The uniform (alternating) bonding orientation yields the $P\bar{1}$ ($Cmca$) structure. An important thing is that the $Im\bar{3}m$-H_3S structure can also be formed with the present unit by binding them so that the vertical edges are shared [Fig. 3(c)].

The unit-based perspective for H_2S and H_3S is indeed helpful for us to construct a group of metastable structures. In a wide variety of materials such as metal oxides, multiple crystalline phases with slightly different stoichiometries emerge depending on the bonding between the unit complexes [35,36]. One such example is the Magnéli phases in molybdenum [20,37,38], tungsten [20,39], titanium [40–43], and vanadium oxides [44–47], where two-dimensional defects (or *crystallographic shear* [48]) of edge- or face-sharing bonding between metal-oxide complexes are periodically formed. In analogy with them, here we consider the possible crystalline phases formed by the structural H_2S unit.

We first define the three types of interunit bonding [Figs. 3(a)–3(c)]: Bonding α and $\bar{\alpha}$ correspond to the two bonding orientations seen in $Cmca$-H_2S, respectively, whereas bonding β corresponds to the bond sharing the edge. With this definition, by arranging the units side by side and next assigning any type of bonding for every neighboring pair of units, we can generate a crystal

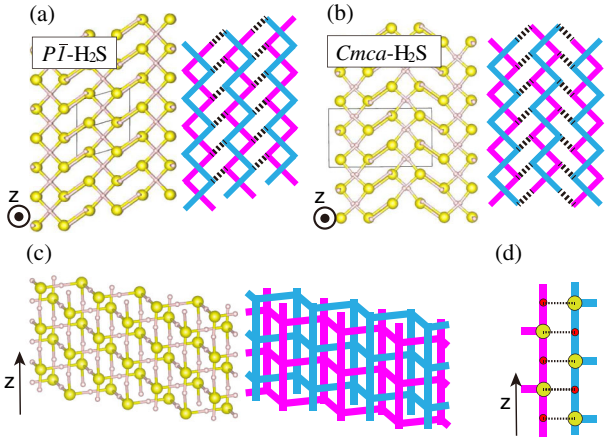

FIG. 2. (a) $(1\ \ 1\ \ 0)$ view of $P\bar{1}$-H_2S and (b) $(1\ \ 0\ \ 0)$ view of $Cmca$-H_2S, accompanied by their schematic pictures. The unit cells are depicted as thin lines. In the schematic pictures, the bond depicted by (d) is indicated by thick dashed lines. (c) The fundamental unit structure, "interlaced square nets" and its schematic picture. In the latter, sulfur and hydrogen atoms are located at the corners and the centers of the edges, respectively. (d) Bonding structure in (a) and (b), where sulfur and hydrogen atoms are depicted in yellow and red, respectively.

structure formed by the units. In this sense, every circular permutation composed of the desired numbers of α, $\bar{\alpha}$, and β yields a corresponding long-period modulated crystal structure. Any structures generated in this way have the intermediate composition H_xS_{1-x} ($2/3 \leq x \leq 3/4$), whose unit cells are composed of $H_{4N-k}S_{2N-k}$ with N and k being the period of the permutation and the number of β, respectively. The "$\alpha\beta\bar{\alpha}\beta$" structure is exemplified in Fig. 3(d), whose unit-cell formula is $H_{14}S_6$. As the number of β increases, H_3S-like structural regions grow [Figs. 3(d) and 3(e)]. Note that $P\bar{1}$-H_2S, $Cmca$-H_2S, and $Im\bar{3}m$-H_3S are generated by permutations "α" (also "$\bar{\alpha}$"; see Supplemental Material [49]), "$\alpha\bar{\alpha}$," and "β," respectively.

Using the structures thus generated from the permutations of periods 2, 3, and 4 as inputs, we carried out the first-principles structure optimization for various pressures. Our calculations were done using the first-principles code package QUANTUM ESPRESSO [52] with the generalized-gradient approximation for the exchange-correlation potential [53]. The unit-cell compositions of the resulting structures are H_7S_3, $H_{10}S_4$, $H_{11}S_5$, $H_{12}S_6$, $H_{13}S_5$, $H_{14}S_6$, $H_{15}S_7$, and $H_{16}S_8$, respectively. Detailed conditions of the calculations are summarized in Supplemental Material [49]. We have found that the formation enthalpy $\Delta H(H_xS_{1-x})$ for all the resulting structures satisfies $\Delta H(H_2S) \gtrsim \Delta H(H_xS_{1-x}) \gtrsim \Delta H(H_3S)$ (Fig. 4). We have also confirmed that all these structures retain the bonding characteristics in their initial structures [Fig. 3(e)]. Namely, every different permutation gives different optimum metastable structures where well-defined bcc-H_3S slab regions emerge. Although we do not examine the $N \geq 5$ cases here,

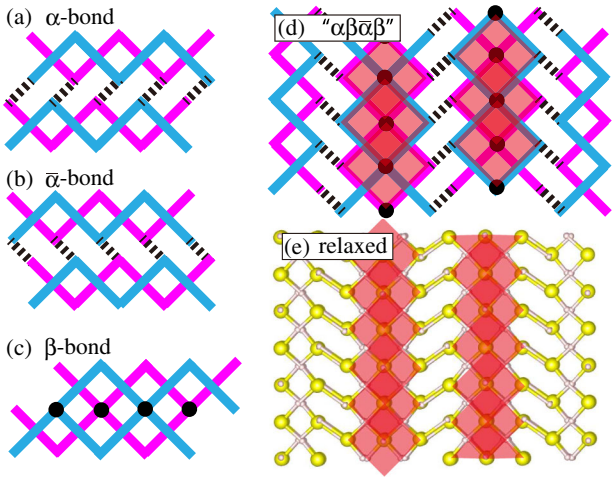

FIG. 3. (a)–(c) Definitions of interunit bonding. (d) Long-period modulated structure generated from permutation "$\alpha\beta\bar{\alpha}\beta$" and (e) its relaxed counterpart (see the main text). The $Im\bar{3}m$-H_3S regions are shaded in red.

an infinite number of metastable structures are expected to be obtained in this way.

Remarkably, the values of the formation enthalpy relative to the complete decomposition into H_2S and H_3S are wholly within 50 K per atom [insets in Figs. 4(a)–4(d)]. This dependence is not an indication of a trivial phase separation into H_2S and H_3S, because the two regions intergrow in a microscopic scale in the respective structures [see Fig. 3(e)]. A more appropriate interpretation is that the formation enthalpy for the H_2S-H_3S boundary is extremely small in these structures.

Let us argue the relevance of the newly found intermediate phases in the experimental situation. We here have to bear in mind that the intermediate structures are *within* the convex hull of the formation enthalpy in the present pressure regime, apart from the narrow range around 110 GPa (Fig. 4 and Ref. [18]). This means that, in the compressed H_2S system, these phases do not grow as the decomposition residues of the emergence of the H_3S phase, if annealed with enough time and heat. However, the decomposition paths otherwise depend on the enthalpy barrier from the pristine H_2S structures. The transition between two metastable structures with slightly different x occurs through transformations of a small fraction of $\alpha(\bar{\alpha})$-type interunit bonds to β. This sporadic character of the bonding transformation and the small formation enthalpy for the H_2S-H_3S boundary revealed above suggest that such a transition requires little activation enthalpy. The intermediate crystalline phases should thus be observable if H_xS systems exhibit either the $P\bar{1}$- or $Cmca$-H_2S region and next further compressed at a low temperature.

The possible emergence of the intermediate Magnéli-type phases draws a consistent explanation of the puzzling pressure dependence of T_c observed experimentally. In the present Magnéli phases, T_c is expected to increase as

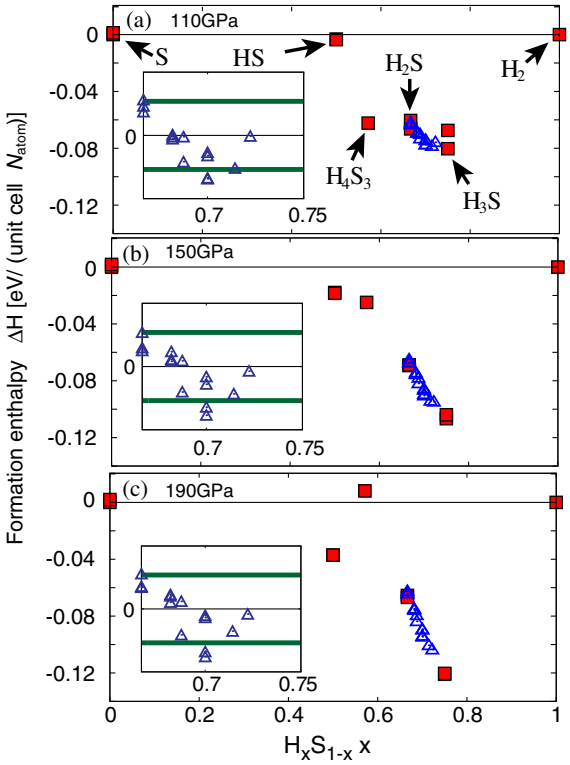

FIG. 4. (a)–(c) Formation enthalpy from first principles at various pressures, where N_{atom} denotes the number of atoms in the unit cell. The structures corresponding to the points are summarized in Supplemental Material [49]. The inset panels focus the region between $x = 2/3$ (H_2S) and $x = 3/4$ (H_3S), where the formation enthalpies are measured with respect to the values for the phase separation of H_2S and H_3S. Bold lines indicate ± 50 K.

the H_3S regions grow. Indeed, by selecting plausible phases and calculating their superconducting T_c's from first principles [13,49,52,56–58,60–62,66,72], we successfully reproduced the experimentally observed T_c behavior (Fig. 1): 41 K (130 GPa), 80 K (180 GPa), 107 K (190 GPa), and 121 K (200 GPa). Here, the increase of T_c is due to the enhancement of electron-phonon coupling (see Supplemental Material [49]). The succession of the Magnéli phases with an increasing fraction of the H_3S region is hence the probable origin of the pressure dependence of T_c observed with the low-T compression scheme, filling the unsolved gap between the theory and experiments. Although we have selected the $\alpha\beta$, $\alpha\beta\beta$, $\alpha\beta\beta\beta$, and $\alpha(\beta \times 9)$ phases for 130, 180, 190, and 200 GPa, respectively, we do not conclude that these specific phases were emerging in the experimental situation in Ref. [1] but were more various Magnéli phases. For example, there has been a recent first-principles calculation that H_5S_2, which is actually equivalent to the $\alpha\beta\beta$ phase, also yields a good agreement for $P <$ 150 GPa (circle with x mark in Fig. 1; Ref. [16]).

We can also find a plausible reaction path consistent with the experiment. The calculated formation enthalpies

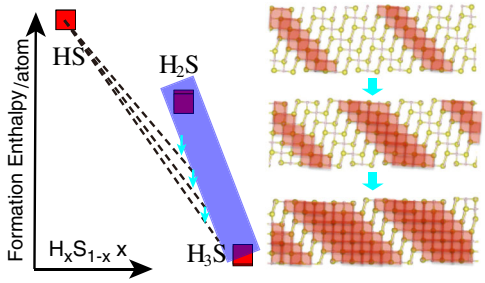

FIG. 5. Schematic picture of a possible transformation path "$\alpha(\bar{\alpha}) \rightarrow \beta + \mathrm{HS}$." The shaded area in the left plot represents the multiple intermediate structures, whereas that in the right indicates the H_3S regions.

for HS and the Magnéli phases decrease with compression compared with those for H_2S [see Figs. 4(a)–4(c)]. This pressure-induced phenomenon would stimulate local reactions forming the H_3S slabs: $\alpha\ (\bar{\alpha}) \rightarrow \beta + \mathrm{HS}$ (Fig. 5; see also Supplemental Material [73]). This supports the present scenario: the increase of the H_3S region by compression.

The multiplicity of the metastable phases deduces an interesting speculation: Arbitrary values of T_c between those of the low- and high-T_c phases in Ref. [1] are observable. The local H_3S-slab formation can also be stimulated by annealing. By carefully controlling the annealing conditions, one would observe various values and their temporal evolution even at fixed pressures.

Here we note a possible characteristic effect in the present H_xS Magnéli phases for future studies. In the titanium-oxide Magnéli phase, it is known that the local electron-lattice coupling is enhanced by two-dimensional defects to form bipolarons (or charge order) [71]. Hydrogen atoms are, in principle, subject to this instability because of their multivalent character. Although we have not found traces of such polaronic phases (see Supplemental Material [49]), in view of the strong electron-phonon coupling, proximity effects of such phases may affect the transport and superconducting properties [74–77].

To facilitate the experimental exploration of the H_xS Magnéli phases, we computed theoretical x-ray diffraction patterns at 150 GPa using the RIETAN package (Ref. [55]; see Supplemental Material [49]). We focus on two distinct groups of structures. When the fraction of the β bond is small and both α and $\bar{\alpha}$ bonds are present, multiple minor peaks are generally seen around the diffraction angle of the dominant peak in $R3m$-H_3S [(110) peak; $2\theta \simeq 11°$ in Fig. 6(a)], as exemplified in Fig. 6(b). This behavior is due to a subtle distortion of the sulfur lattice and apparently difficult to understand with a simple combination of the patterns for the pristine $R3m$-H_3S, $P\bar{1}$-H_2S, and $Cmca$-H_2S phases. Experimental "noise" may actually be contributed to by the diffraction peaks from those phases. We also show the simulated patterns when the β bonds are gradually introduced in either the $P\bar{1}$- or $Cmca$-H_2S phase in Fig. 6(c). We observe gradual evolutions between the end

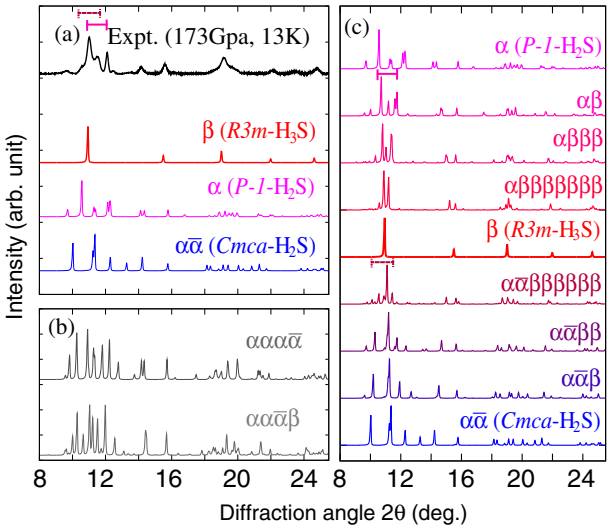

FIG. 6. X-ray diffraction patterns. The simulations were done for the structures optimized at 150 GPa. (a) (Top) Experimentally observed diffraction pattern for D_2S taken from Ref. [8], where the horizontal bars indicate regions where we can find a similarity to the simulated patterns for some Magnéli phases [see (c)]. (Bottom) The simulated patterns for the reference structures. (b) Representative simulated patterns exhibiting multiple diffraction peaks. (c) Patterns obtained from a selected group of structures which are ordered so that the fraction of β bond gradually varies.

points. Remarkably, the intensity of the dominant peak is well retained, while peripheral features such as subpeaks and a peak shift and tail are found. In the previous diffraction experiments [8,18,32], the presence of the H_3S phase has been indicated from the (110) peak, though it was accompanied by subtle subpeaks depending on the experimental protocol. The Magnéli phases of this group may provide a unified understanding of such structures. To demonstrate this, we plotted an experimental pattern quoted from Ref. [8] in Fig. 6(a). The subpeaks and tails around $10° \lesssim 2\theta \lesssim 12°$ well resembles, for example, those for $\alpha\beta$ and $\alpha\bar{\alpha}\beta\beta\beta\beta\beta\beta$, as indicated in Figs. 6(a) and 6(c).

We additionally assert that not only crystalline Magnéli phases but also their nanoscale stripes can emerge in an ordered and random fashion, similarly to the cases of microsyntactic intergrowth [45] observed in silicon carbide [78] and metallic oxides including the Magnéli materials [45,79–82]. Such structures will appear in reality as an alloylike phase formed by the slabs of the metallic H_2S and H_3S. This alloy phase is a compound analog of the classic superconducting alloys formed by elemental metals [83] but quite different from them. The ingredients of the former alloy—H_2S and H_3S slabs—can develop in the common H_2S crystalline phases, and therefore, even in the pristine sample, their alloying occurs in a self-contained manner through structural and stoichiometric transformations. This alloying obviously smears the experimental diffraction pattern, which could appear to be amorphouslike behavior.

In summary, we have provided an interpretation based on the common structural unit for the known crystal structures of low- and high-T_c H_2S and H_3S and thereby found metastable Magnéli-type structures formed by their layered microsyntactic intergrowth. The experimentally observed pressure dependence of T_c is reasonably explained with pressure-induced gradual transformations through such alloy phases. The present finding gives new insight into the high-T_c superconducting phenomena in sulfur hydride that the microscopic mixture of the phases can be ubiquitous.

This work was supported by MEXT Element Strategy Initiative to Form Core Research Center in Japan and JSPS KAKENHI Grants No. 15K20940 (R. Akashi) and No. 15H03696 (R. Arita) from Japan Society for the Promotion of Science (JSPS). We thank Yinwei Li and Mari Einaga for sharing structure data for H_4S_3 in Ref. [18] and x-ray diffraction data in Ref. [8], respectively. We also thank Mikhail Eremets, Yoshihiro Iwasa, Hui-hai Zhao, and Yuta Tanaka for enlightening comments. The crystal structures were depicted using VESTA [84]. The superconducting properties were calculated at the Supercomputer Center at the Institute for Solid State Physics in the University of Tokyo.

*akashi@cms.phys.s.u-tokyo.ac.jp

[1] A. P. Drozdov, M. I. Eremets, I. A. Troyan, V. Ksenofontov, and S. I. Shylin, Nature (London) **525**, 73 (2015).
[2] A. P. Drozdov, M. I. Eremets, and I. A. Troyan, arXiv: 1412.0460.
[3] J. Bardeen, L. N. Cooper, and J. R. Schrieffer, Phys. Rev. **108**, 1175 (1957).
[4] C. W. Chu, L. Gao, F. Chen, Z. J. Huang, R. L. Meng, and Y. Y. Xue, Nature (London) **365**, 323 (1993).
[5] L. Gao, Y. Y. Xue, F. Chen, Q. Xiong, R. L. Meng, D. Ramirez, C. W. Chu, J. H. Eggert, and H. K. Mao, Phys. Rev. B **50**, 4260(R) (1994).
[6] M. Monteverde, C. Acha, M. Núñez-Regueiro, D. A. Pavlov, K. A. Lokshin, S. N. Putilin, and E. V. Antipov, Europhys. Lett. **72**, 458 (2005).
[7] N. Takeshita, A. Yamamoto, A. Iyo, and H. Eisaki, J. Phys. Soc. Jpn. **82**, 023711 (2013).
[8] M. Einaga, M. Sakata, T. Ishikawa, K. Shimizu, M. I. Eremets, A. P. Drozdov, I. A. Troyan, N. Hirao, and Y. Ohishi, arXiv:1509.03156 [Nat. Phys (to be published)].
[9] Y. Li, J. Hao, H. Liu, Y. Li, and Y. Ma, J. Chem. Phys. **140**, 174712 (2014).
[10] D. Duan, Y. Liu, F. Tian, D. Li, X. Huang, Z. Zhao, H. Yu, B. Liu, W. Tian, and T. Cui, Sci. Rep. **4**, 6968 (2014).
[11] N. Bernstein, C. S. Hellberg, M. D. Johannes, I. I. Mazin, and M. J. Mehl, Phys. Rev. B **91**, 060511(R) (2015).
[12] J. A. Flores-Livas, A. Sanna, and E. K. U. Gross, Eur. Phys. J. B **89**, 63 (2016).
[13] R. Akashi, M. Kawamura, S. Tsuneyuki, Y. Nomura, and R. Arita, Phys. Rev. B **91**, 224513 (2015).
[14] I. Errea, M. Calandra, C. J. Pickard, J. Nelson, R. J. Needs, Y. Li, H. Liu, Y. Zhang, Y. Ma, and F. Mauri, Phys. Rev. Lett. **114**, 157004 (2015).
[15] I. Errea, M. Calandra, C. J. Pickard, J. R. Nelson, R. J. Needs, Y. Li, H. Liu, Y. Zhang, Y. Ma, and F. Mauri, Nature (London) **532**, 81 (2016).
[16] T. Ishikawa, A. Nakanishi, K. Shimizu, H. Katayama-Yoshida, T. Oda, and N. Suzuki, Sci. Rep. **6**, 23160 (2016).
[17] W. Sano, T. Koretsune, T. Tadano, R. Akashi, and R. Arita, Phys. Rev. B **93**, 094525 (2016).
[18] Y. Li, L. Wang, H. Liu, Y. Zhang, J. Hao, C. J. Pickard, J. R. Nelson, R. J. Needs, W. Li, Y. Huang, I. Errea, M. Calandra, F. Mauri, and Y. Ma, Phys. Rev. B **93**, 020103(R) (2016).
[19] D. Duan, X. Huang, F. Tian, D. Li, H. Yu, Y. Liu, Y. Ma, B. Liu, and T. Cui, Phys. Rev. B **91**, 180502(R) (2015).
[20] A. Magnéli, Acta Crystallogr. **6**, 495 (1953).
[21] D. A. Papaconstantopoulos, B. M. Klein, M. J. Mehl, and W. E. Pickett, Phys. Rev. B **91**, 184511 (2015).
[22] Y. Quan and W. E. Pickett, Phys. Rev. B **93**, 104526 (2016).
[23] E. J. Nicol and J. P. Carbotte, Phys. Rev. B **91**, 220507 (2015).
[24] C. Heil and L. Boeri, Phys. Rev. B **92**, 060508(R) (2015).
[25] M. Komelj and H. Krakauer, Phys. Rev. B **92**, 205125 (2015).
[26] A. Bianconi and T. Jarlborg, Nov. Supercond. Mater. **1**, 37 (2015).
[27] A. Bianconi and T. Jarlborg, Europhys. Lett. **112**, 37001 (2015).
[28] T. Jarlborg and A. Bianconi, Sci. Rep. **6**, 24816 (2016).
[29] L. Ortenzi, E. Cappelluti, and L. Pietronero, arXiv: 1511.04304.
[30] A. P. Durajski, R. Szczęśniak, and L. Pietronero, Ann. Phys. (Berlin) **528**, 358 (2016).
[31] L. P. Gor'kov and V. Z. Krezin, Sci. Rep. **6**, 25608 (2016).
[32] A. F. Goncharov, S. S. Lobanov, I. Kruglov, X.-M. Zhao, X.-J. Chen, A. R. Oganov, Z. Konôpková, and V. B. Prakapenka, Phys. Rev. B **93**, 174105 (2016).
[33] Note that the theoretically predicted $R3m$ distortion is so small as to be difficult to measure in the experiment.
[34] We can also regard that the dominant interunit bonding is the S-S one [9] instead of S-H, though this difference does not change the conclusion of the later discussions.
[35] L. Bragg and G. F. Claringbull, *Crystal Structure of Minerals* (Bell, London, 1965).
[36] L. R. Eyring and L. T. Tai, in *Crystalline and Noncrystalline Solids*, edited by N. B. Hannay, Treatise on Solid State Chemistry Vol. 3 (Plenum, New York, 1976), Chap. 3.
[37] L. A. Bursill, Proc. R. Soc. A **311**, 267 (1969).
[38] D. Wang, D. Su, and R. Schlögl, Cryst. Res. Technol. **38**, 153 (2003).
[39] M. Sundberg and R. J. D. Tilley, Phys. Status Solidi A **22**, 677 (1974); R. Pickering and R. J. D. Tilley, J. Solid State Chem. **16**, 247 (1976).
[40] S. Andersson, B. Collén, U. Kuylenstierna, and A. Magnéli, Acta Chem. Scand. **11**, 1641 (1957); S. Andersson, B. Collén, G. Kruuse, U. Kuylenstierna, A. Magnéli, H. Pestmalis, and S. Åsbrink, Acta Chem. Scand. **11**, 1653 (1957).
[41] O. Terasaki and D. Watanabe, Jpn. J. Appl. Phys. **10**, 292 (1971).

[42] L. A. Bursill and B. G. Hyde, Prog. Solid State Chem. **7**, 177 (1972).
[43] S. Harada, K. Tanaka, and H. Inui, J. Appl. Phys. **108**, 083703 (2010).
[44] S. Andersson and L. Jahnberg, Ark. Kemi **21**, 413 (1963).
[45] Y. Hirotsu, Y. Tsunashima, S. Nagakura, H. Kuwamoto, and H. Sato, J. Solid State Chem. **43**, 33 (1982).
[46] P. C. Canfield, J. D. Thompson, and G. Gruner, Phys. Rev. B **41**, 4850(R) (1990).
[47] U. Schwingenschlögl and V. Eyert, Ann. Phys. (Berlin) **13**, 475 (2004).
[48] A. D. Wadsley, in *Fasciculus Extraordinarius Alfred Werner, 1866-1919: Alfred Werner Commemoration Volume* (Verlag Helvetica Chimica Acta, Basel, 1967).
[49] See Supplemental Material at http://link.aps.org/supplemental/10.1103/PhysRevLett.117.075503 for equivalence of the bonding permutations, details of the first-principles calculations of optimized structures, electronic density of states and superconducting properties, investigation of charge imbalance and possible local reactions forming H_3S slabs, which include Refs. [50–71].
[50] O. Degtyareva, E. Gregoryanz, M. Somayazulu, H. K. Mao, and R. J. Hemley, Phys. Rev. B **71**, 214104 (2005).
[51] C. J. Pickard and R. J. Needs, Nat. Phys. **3**, 473 (2007).
[52] P. Giannozzi *et al.*, J. Phys. Condens. Matter **21**, 395502 (2009); http://www.quantum-espresso.org/.
[53] J. P. Perdew, K. Burke, and M. Ernzerhof, Phys. Rev. Lett. **77**, 3865 (1996).
[54] N. Troullier and J. L. Martins, Phys. Rev. B **43**, 1993 (1991); http://www.abinit.org/downloads/psp-links/psp-links/gga_fhi.
[55] F. Izumi and K. Momma, Solid State Phenom. **130**, 15 (2007).
[56] M. Lüders, M. A. L. Marques, N. N. Lathiotakis, A. Floris, G. Profeta, L. Fast, A. Continenza, S. Massidda, and E. K. U. Gross, Phys. Rev. B **72**, 024545 (2005).
[57] M. A. L. Marques, M. Lüders, N. N. Lathiotakis, G. Profeta, A. Floris, L. Fast, A. Continenza, E. K. U. Gross, and S. Massidda, Phys. Rev. B **72**, 024546 (2005).
[58] R. Akashi and R. Arita, Phys. Rev. B **88**, 014514 (2013).
[59] Y. Takada, J. Phys. Soc. Jpn. **45**, 786 (1978).
[60] R. Akashi and R. Arita, Phys. Rev. Lett. **111**, 057006 (2013).
[61] R. Akashi and R. Arita, J. Phys. Soc. Jpn. **83**, 061016 (2014).
[62] S. Baroni, S. de Gironcoli, A. Dal Corso, and P. Giannozzi, Rev. Mod. Phys. **73**, 515 (2001).
[63] D. Pines, *Elementary Excitations in Solids* (Benjamin, New York, 1963).
[64] R. Akashi, K. Nakamura, R. Arita, and M. Imada, Phys. Rev. B **86**, 054513 (2012).
[65] M. Methfessel and A. T. Paxton, Phys. Rev. B **40**, 3616 (1989).
[66] M. Kawamura, Y. Gohda, and S. Tsuneyuki, Phys. Rev. B **89**, 094515 (2014).
[67] J. Rath and A. J. Freeman, Phys. Rev. B **11**, 2109 (1975).
[68] P. E. Blöchl, O. Jepsen, and O. K. Andersen, Phys. Rev. B **49**, 16223 (1994).
[69] P. B. Allen and R. C. Dynes, Phys. Rev. B **12**, 905 (1975).
[70] G. Henkelman, A. Arnaldsson, and H. Jónsson, Comput. Mater. Sci. **36**, 354 (2006); E. Sanville, S. D. Kenny, R. Smith, and G. Henkelman, J. Comput. Chem. **28**, 899 (2007); W. Tang, E. Sanville, and G. Henkelman, J. Phys. Condens. Matter **21**, 084204 (2009).
[71] S. Lakkis, C. Schlenker, B. K. Chakraverty, R. Buder, and M. Marezio, Phys. Rev. B **14**, 1429 (1976).
[72] A. B. Migdal, Zh. Eksp. Teor. Fiz. **34**, 1438 (1958) [Sov. Phys. JETP **7**, 996 (1958)]; G. M. Eliashberg, Zh. Eksp. Teor. Fiz. **38**, 966 (1960) [Sov. Phys. JETP **11**, 696 (1960)]; D. J. Scalapino, in *Superconductivity*, edited by R. D. Parks (Marcel Dekker, New York, 1969), Vol. 1; J. R. Schrieffer, *Theory of Superconductivity; Revised Printing* (Westview Press, Boulder, CO, 1971).
[73] We can also consider another possible reaction forming local H_3S slabs and stimulated by compression: $\alpha(\bar{\alpha}) + H_2 \rightarrow 2\beta$ [49].
[74] B. K. Chakraverty, J. Phys. (Paris) **40**, L99 (1979); **42**, 1351 (1981).
[75] A. S. Alexandrov, Zh. Fi. Khim. **57**, 273 (1983).
[76] A. S. Alexandrov and J. Ranninger, Phys. Rev. B **24**, 1164 (1981); A. S. Alexandrov, J. Ranninger, and S. Robaszkiewicz, Phys. Rev. B **33**, 4526 (1986).
[77] A. S. Alexandrov and N. F. Mott, Rep. Prog. Phys. **57**, 1197 (1994); J. T. Devreese and A. S. Alexandrov, Rep. Prog. Phys. **72**, 066501 (2009).
[78] H. Sato and S. Shiozaki, Mater. Res. Bull. **9**, 679 (1974).
[79] D. J. M. Bevan, B. Hudson, and P. T. Moseley, Mater. Res. Bull. **9**, 1073 (1974).
[80] Y. Hirotsu and H. Sato, J. Solid State Chem. **26**, 1 (1978).
[81] Y. Hirotsu, S. P. Faile, and H. Sato, Mater. Res. Bull. **13**, 895 (1978).
[82] Y. Hirotsu and H. Sato, Mater. Res. Bull. **15**, 41 (1980).
[83] B. T. Matthias, T. H. Geballe, and V. B. Compton, Rev. Mod. Phys. **35**, 1 (1963).
[84] K. Momma and F. Izumi, J. Appl. Crystallogr. **44**, 1272 (2011).